We are IntechOpen, the world's leading publisher of Open Access books
Built by scientists, for scientists

5,300
Open access books available

130,000
International authors and editors

155M
Downloads

Our authors are among the

154
Countries delivered to

TOP 1%
most cited scientists

12.2%
Contributors from top 500 universities

CLARIVATE ANALYTICS
BOOK CITATION INDEX
INDEXED

WEB OF SCIENCE™

Selection of our books indexed in the Book Citation Index
in Web of Science™ Core Collection (BKCI)

Interested in publishing with us?
Contact book.department@intechopen.com

SOA-Based Optical Packet Switching Architectures

V. Eramo[1], E. Miucci[1], A. Cianfrani[1], A. Germoni[2] and M. Listanti[1]
[1]*DIET Sapienza University of Rome,*
[2]*Co.Ri.Tel.*
Italy

1. Introduction

The service evolution and the rapid increase in traffic levels fuel the interest toward switching paradigms enabling the fast allocation of Wavelength Division Multiplexing WDM channels in an on demand fashion with fine granularities (microsecond scales). For this reason, in the last years, different optical switching paradigms have been proposed (Sabella et al., 2000): optical-packet switching (OPS), optical-burst switching (OBS), wavelength-routed OBS, etc. Among the various all-optical switching paradigms, OPS attracts increasing attention. Owing to the high switching rate, Semiconductor Optical Amplifier (SOA) is a key technology to realize Optical Packet Switches. We propose some Optical Packet Switch (OPS) architectures and illustrate their realization in SOA technology. The effectiveness of the technology in reducing the power consumption is also analyzed. The chapter is organized in three sections. The main blocks (Switching Fabric, Wavelength Conversion stage, Synchronization stage) of an OPS are illustrated in Section 2 where we also show some examples of realizing wavelength converters and synchronizers in SOA technology. Section 3 introduces SOA-based single-stage and multi-stage switching fabrics. Finally the SOA-based OPS power consumption is investigated in Section 4.

2. Optical packet switching architectures

The considered optical switch architecture (Eramo, 2000; 2006; Sabella et al., 2000) is shown in Fig. 1. It has N input and output fibers, each fiber supports a WDM signal with M wavelengths, so an input (or output) channel is characterized by the couple (i, λ_j) wherein i ($i \in 1, \cdots, N$) identifies the input/output fiber and λ_j, ($j \in 1, \ldots, M$) identifies the wavelength. In general, optical packet switches can be divided into two categories: slotted (synchronous) and unslotted (asynchronous) networks. In a synchronous switch (Eramo, 2000), as illustrated in Fig. 1 packets with fixed length are aligned (synchronized) by synchronizers before they enter the switch fabric. This type of switch generally achieves a fairly good throughput since the behavior of the packets is regulated. However, complex and expensive synchronization hardware is needed at each node. On the other hand, in an asynchronous switch (Eramo et al., 2003), the packets are not aligned and they are switched one by one on the fly. Asynchronous networks generally have lower cost, better flexibility, and robustness, but usually they have lower overall throughput than synchronous networks. The switch architecture is equipped with a number r of WCs which are shared according

are composed of a series of optical switches designed to select the proper optical path and pairs of fiber delay lines with different optical lengths of $\frac{T_s}{2^k}$ (T_s:time slot; k:integer). In these architectures, however, increasing the number of switches to improve the time resolution causes additional increases in optical loss and crosstalk. To overcome loss problems SOA-based synchronizers have been proposed. Next we illustrate and explain two of them. In the first one (Sakamoto et al., 2002) synchronization is achieved by selecting one of some optical paths, each with a different length, using wavelength and space switching based on a wavelength-tunable distributed Bragg reflector laser diode (LD) and n semiconductor optical amplifier (SOA) gates per channel. The synchronizer has its own internal reference clock. The clock period equals the time slot duration (T_s) and the synchronizer aligns input packets with the time slot packet by packet. Synchronization is achieved by counting each delay of each input packet with respect to the reference time and choosing the optical paths with the appropriate length. Fig. 2 shows the schematic structure of the synchronizer. Each channel is equipped with a wavelength-divisionmultiplexing (WDM) coupler, a wavelength converter, an optical splitter, semiconductor optical amplifier (SOA) gates, two stages of fiber delay lines, an optical coupler, arrayed waveguide gratings (AWGs) for MUX/DEMUX, a delay counter, and a wavelength-tunable laser. The out-of-band optical label switching technique is used, in which optical packet and optical labels are carried on different wavelengths (Okada et al., 2001). The delay counter estimates the delay of each optical label and selects one of m wavelengths of the tunable laser and one of n SOA gates. The wavelength of each optical packet signal is converted to the laser wavelength by the wavelength converter. The wavelength-converted optical packet signal passes through one of n SOA gates and the first-stage delay lines, each of which has a different delay time of $\frac{T_s}{n}$. The packet signal then passes through one of m AWG ports and the second-stage delay lines, each with delay time difference of $\frac{T_s}{n \times m}$. Consequently, there are optical paths with different lengths and synchronization is attained.

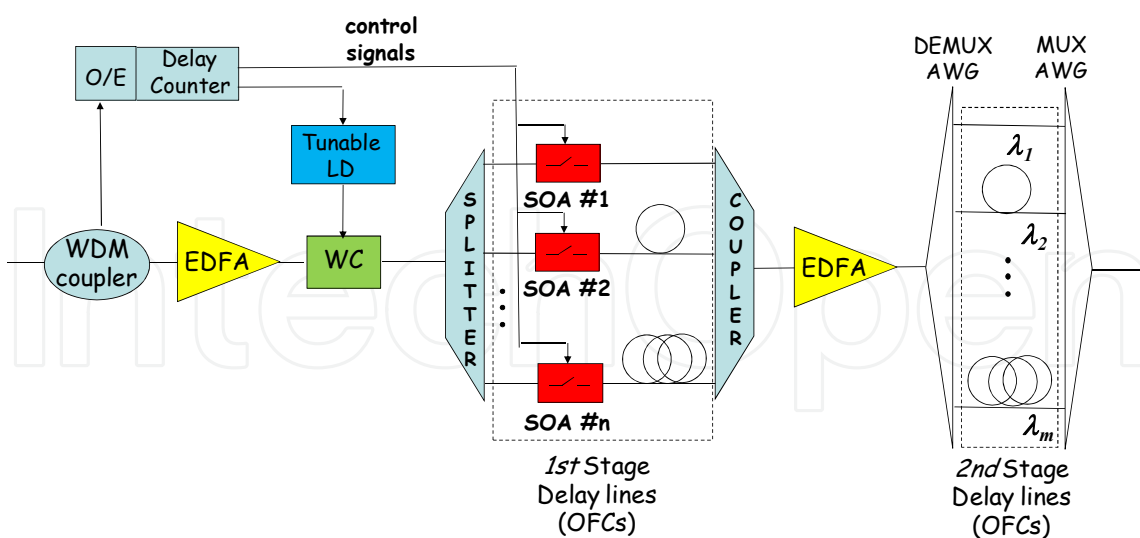Fig. 2. Schematic structure of the synchronizer. WC: Wavelength converter. SOAG: SOA gate. OFC: Optical fiber circuit.

The second synchronizer has been proposed in (Mack et al., 2008) and it is illustrated in Fig. 3. Feed-forward structure with SOA-based gates is used here because of its high operation speed, large tuning range, and the potential for integration within the large SOA-based switch

(Mack et al., 2008). The synchronizer is composed by N_{SYN} stages. There are one 1×2 splitter, one 2×1 coupler, two SOAs, two optical bandpass filter(OBF) and one FDL in each stage. SOAs were used as the gates to select the required delay and compensate for losses. In order to suppress accumulated amplified spontaneous emission, Optical Bandpass Filters was placed inside each synchronizations stage.
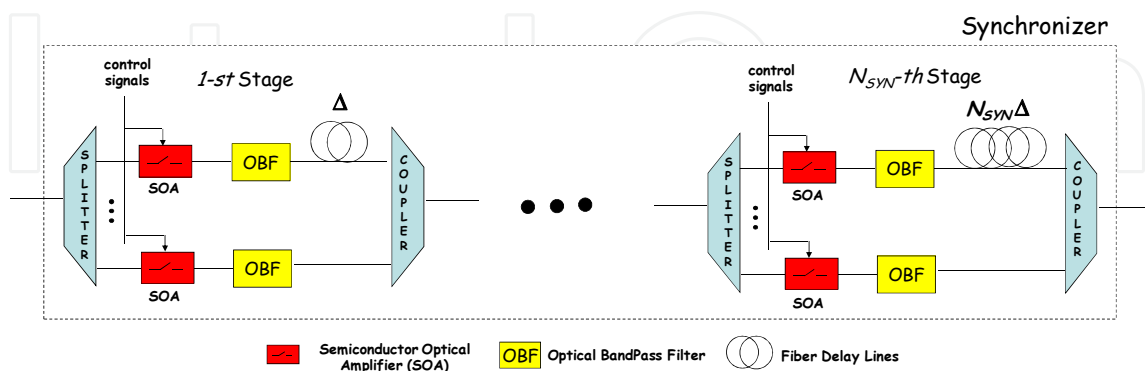
Fig. 3. Fiber based synchronizer with SOA gates and Optical Bandpass Filter (OBF). Δ is the delay introduced by the fiber delay line of the 1st stage.

2.2 Realization of SOA-based Wavelength Converters

In packet switching networks, tuneable wavelength converters can be used to resolve packet contention and overcome the optical buffering problem. An example of SOA-based Wavelength Converter is illustrated in Fig. 4. It is referred to as Delayed Interference Signal WCs (DISCs) and has been proposed in (Sakaguchi et al., 2007). DISC employs nonlinear effect in SOA and utilizes an SOA and an OBF placed at the amplifier output. It can be constructed by using commercially available fiber-pigtailed components. It has a simple configuration and allows photonic integration.

Fig. 4. Realization of an all-optical wavelength converter by using a Delayed-Interference Signal Wavelength Converter (DISC).

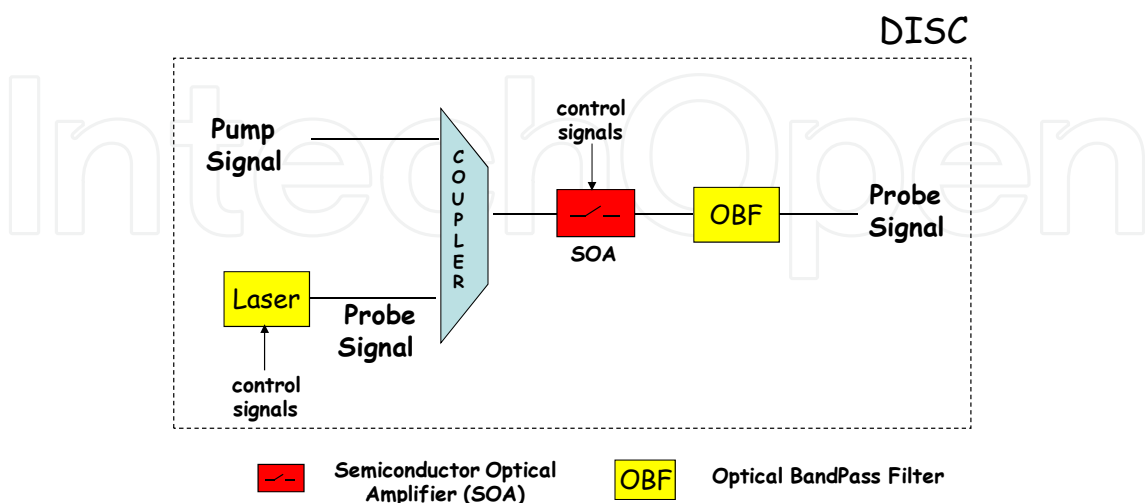## 3. SOA-based switching fabric

Switching fabric in Future Optical Packet Switches require high-speed optical switches (or gates). That can either be optically or electrically controlled. Such optical switches can be constructed using SOAs due to their high switching rate. The simplest method to control an SOA gate is by turning the device current on or off. The great advantage of SOA gates is that they can be integrated to form gate array. Next we illustrate SOA-based Single-Stage and Multi-Stage switching in Sections 3.1 and 3.2 respectively.

3.1 Single-stage approach

The structure of a switching fabric depends on the adopted sharing strategy of the Wavelength Converters. Two of them are reported in Figs 5 and 6.
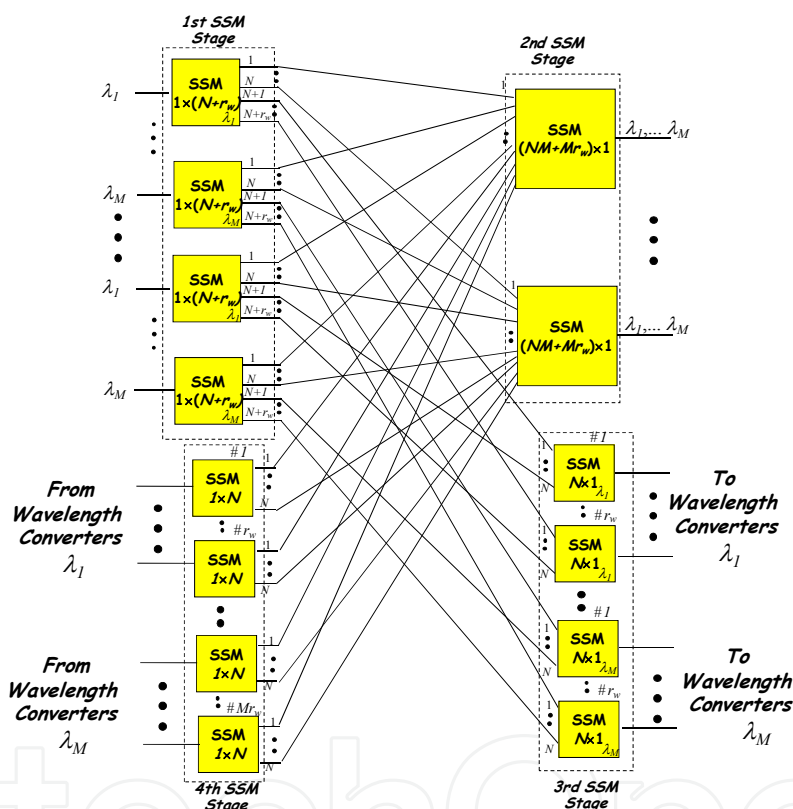
Fig. 5. Shared-Per-Wavelength Single-Stage Optical Switching Fabric.

They are related to two proposed main WC sharing strategies. In the first one, referred to as Shared-Per-Wavelength (SPW) (Eramo et al., 2008; 2009a;b), the WCs are partially shared. All of the packets arriving on a given wavelength share the same pool of converters. In the second one referred to as Shared-Per-Node (SPN) (Eramo et al., 2009c; Eramo, 2010),the WCs are fully shared and all of the arriving packets share the same pool of WCs. Next we illustrate the switching fabrics of the SPW and SPN switches.

The SPW switching fabric is illustrated in 5 and its operation mode is the following (Eramo et al., 2008; 2009a;b). A packet not requiring wavelength conversion is directly routed towards the Output Fibers (OF). On the contrary a packet needing the use of a WC will be directed to the pool of r_w WCs dedicated for the wavelength on which the packet is arriving.

Fig. 6. Shared-Per-Node Single-Stage Optical Switching Fabric.

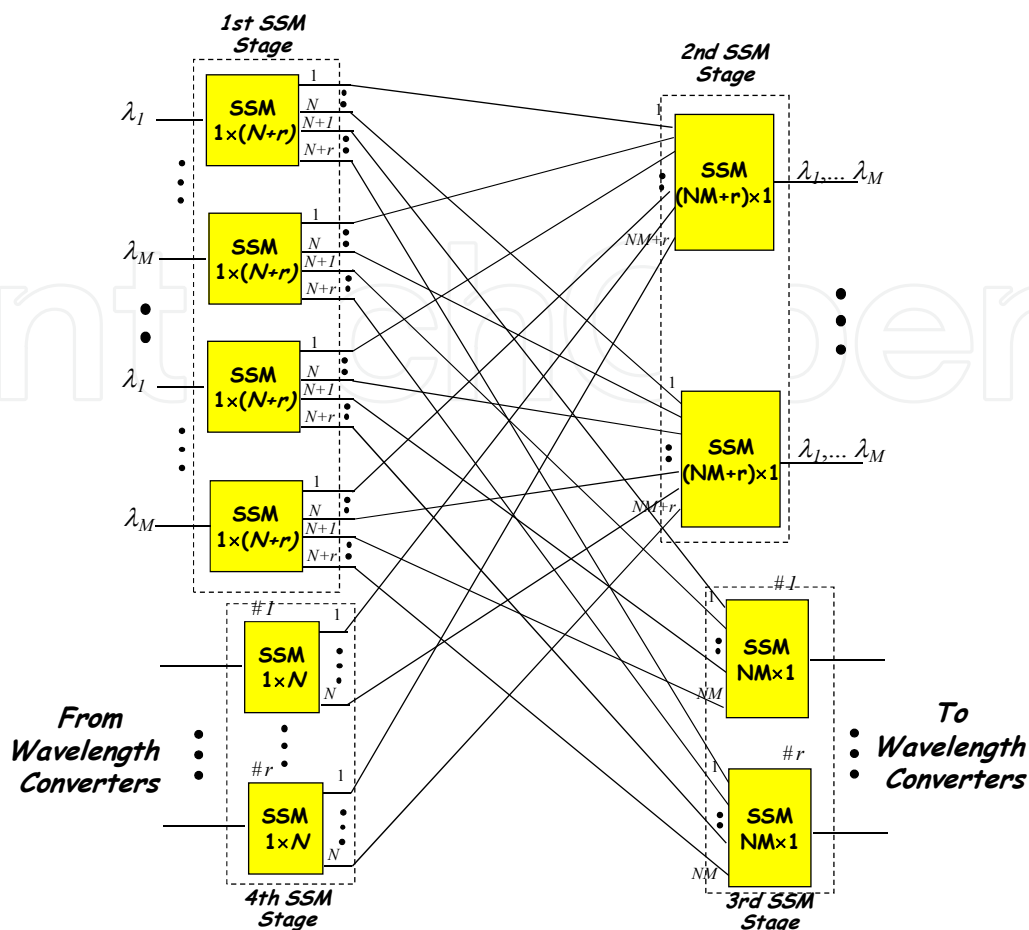The selection of either an OF or a WC is realized by means of a $1 \times (N + r_w)$ Space Switching Module (SSM) of the $1st$ SSM stage. Each $N \times 1$ SSM of the $3rd$ SSM stage in Fig. 5 has the function to forward to a WC the packet selected by the control unit to be wavelength converted. After the conversion, the packets are sent to the OFs by means of a $1 \times N$ SSM of the $4th$ SSM stage. The function of an $(N + r_w)M \times 1$ SSM of the $2nd$ SSM stage is to couple all of the packets directed to any OF.

The SPW sharing strategy (Eramo et al., 2009c; Eramo, 2010) allows for a reduction in the switching fabric complexity, improving the scalability. As a matter of fact, the SSMs of the $1st$ and $3rd$ stage have reduced complexity with respect to the ones of the SPN reference switch diagrammed in Fig. 6 with r denoting the total number of shared WCs. This is due to the fact that r_w, number of WCs shared per wavelength in SPW switch, is much smaller than r, the number of WC shared in SPN switch. The reduction in switching fabric complexity of the SPW switch leads to a smaller signal attenuation and consequently to a smaller SSM power consumption.

We report in Fig. 7.a and Fig. 7.b an example of realization of $1 \times K$ SSM and $K \times 1$ SSM respectively by means of splitters, couplers and Semiconductor Optical Amplifiers (SOA). The input of an $1 \times K$ SSM is switched to the output #j by turning on SOA #j and turn off the remaining SOAs. The SOA in the $K \times 1$ SSM is activated when at least one input signal has to be coupled.
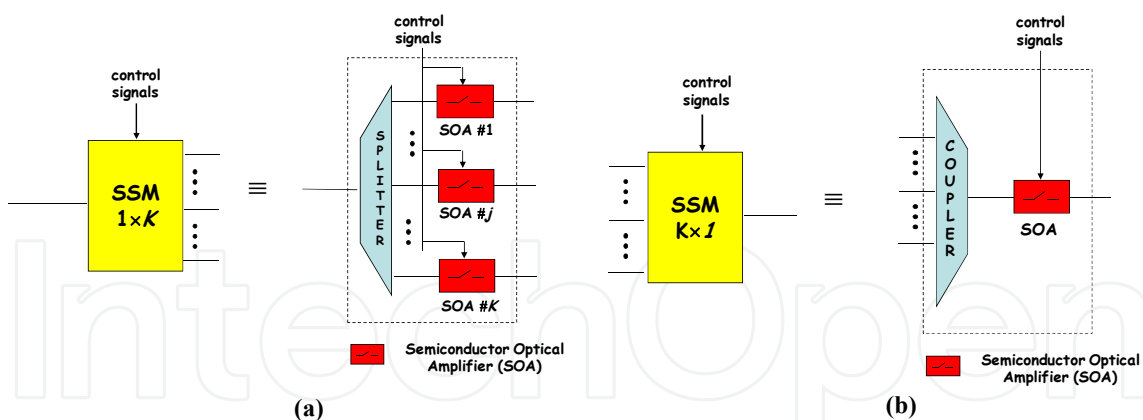
Fig. 7. Realization of $1 \times K$ SSM (a) and $K \times 1$ SSM (b) by means of splitters, couplers and Semiconductor Optical Amplifiers (SOA).

3.2 Multi-stage approach

One of the most used Multi-Stage (MS) switching fabric is the BENES one. It belongs to a class of rearrangeably non blocking networks with 2×2 switching elements. Fig. 8.a shows a 8×8 BENES switch using 20 2×2 switching elements. It is one of the most efficient architectures in terms of used number of 2×2 switching elements. A $P \times P$ BENES switch requires $\frac{P}{2}(2log_2 P - 1)$ 2×2 switching elements, with P being a power of 2 (Benes, 1965). A single 2×2 switch can be realized in SOA technology as shown in Fig. 8.b. It is made by four SOAs, two splitters and two couplers and enables connectivity in both the *bar* and *crossed* states similar to a directional coupler fabricated in lithium niobate.
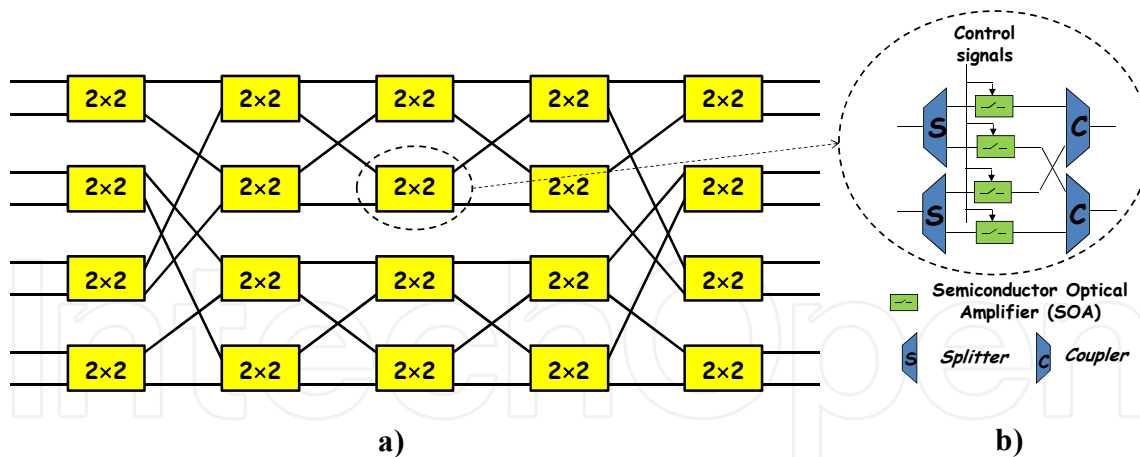
Fig. 8. 8×8 BENES switching architecture realized with 20 2×2 switching elements (a). SOA technology based 2×2 switching element (b).

A switching fabric supporting N IF/OF, M wavelengths and fully shared r wavelength converters can be realized with an $2NM \times 2NM$ BENES network. An example of BENES switching fabric is illustrated in Fig. 9 in the case N=2, M=2 and r=2.

The total number of splitters and couplers can be reduced as illustrated in the switch of Fig. 10. It is obtained by starting from the switch reported in Fig. 9 and by combining in the
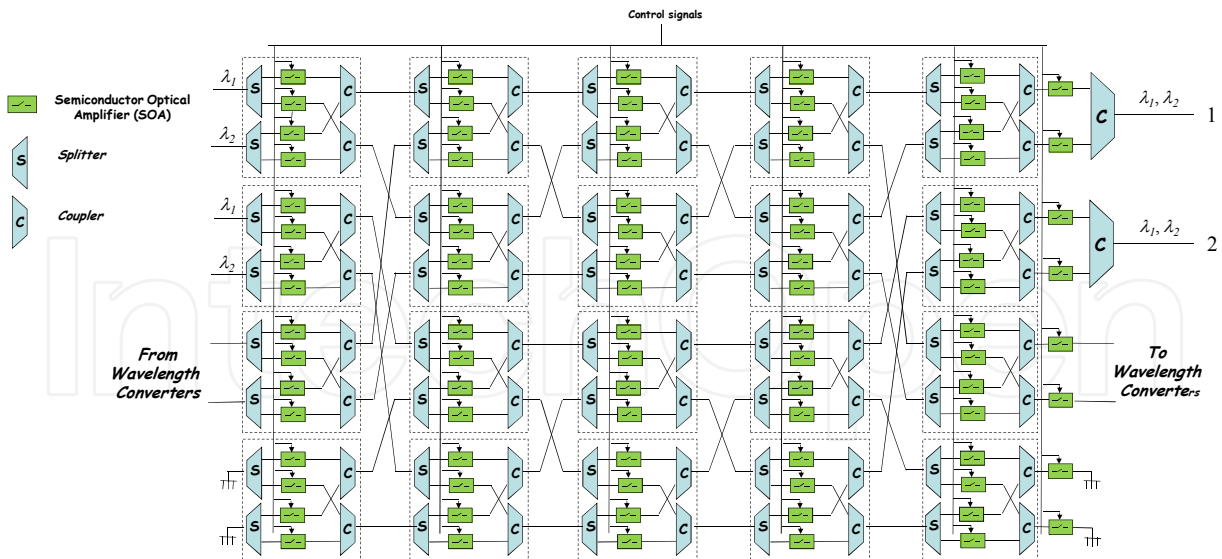
Fig. 9. BENES Optical Packet Switch realized with splitters, couplers and SOAs (N=2, M=2, r=2).

adjacent stages with a 3dB Directional Coupler (DC) the output couplers on the left-hand and the input splitters on the right-hand.
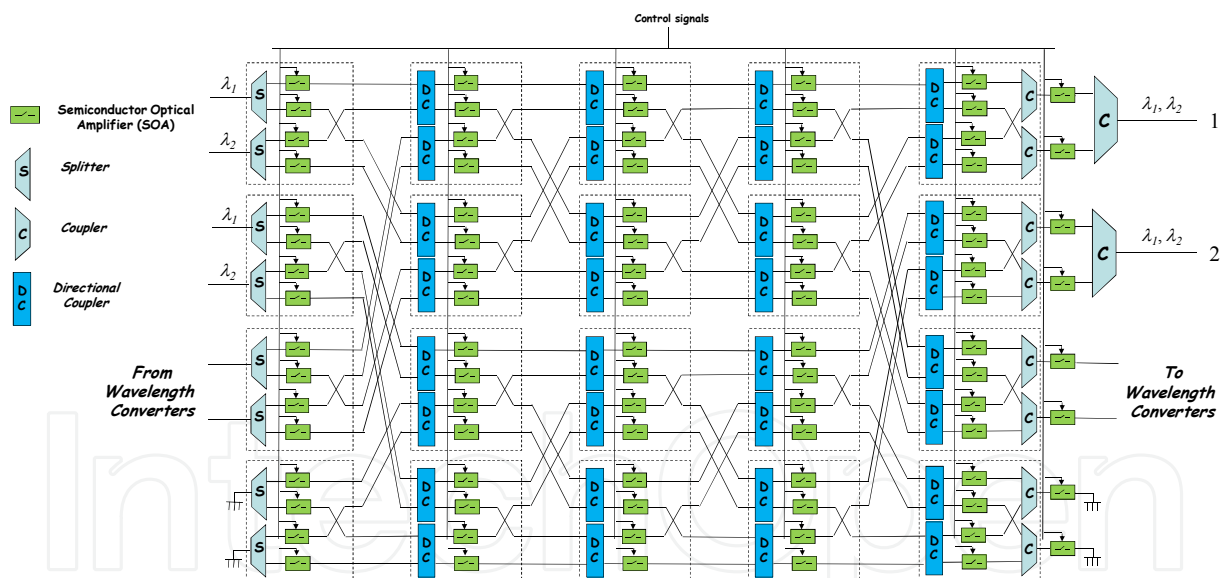
Fig. 10. BENES Optical Packet Switch realized with splitters, directional couplers, couplers and SOAs (N=4, M=2, r=2).

4. Power consumption in SOA-based optical packet switches

High capacity routers system designer are facing with power consumption issues. Today commercial products that can follow the increase in capacity demand for packet switched networks are based on multirack equipment. Optical packet switching (OPS) (Ben Yoo, 2011) systems could lead to solve this issue providing a solution that could be compact, fast, and power efficient. Next we propose some models to investigate the power consumption

of Optical Packet Switching. First of all we introduce a SOA's power consumption model in Section 4.1 able to evaluate the power consumption as a function of the main SOA's parameters (current, forward polarization voltage, material loss, gain,···). Analytical models are introduced in Section 4.2 to evaluate the power consumption of Synchronous SPN (SSPN) Optical Packet Switches equipped with SS and MS switching fabric. Similar models have been introduced for the asynchronous case (Eramo et al., 2009c; Eramo, 2010) and when the SPW sharing strategy is adopted (Akar et al., 2011; Eramo et al., 2011). Some numerical results reporting the power consumption of Optical Packet Switches are illustrated in Section 4.3.

4.1 SOA's power consumption model

The SOA's power consumption model illustrated in (Hinton et al., 2008) is adopted; the SOA's power consumption equals the supply power $P_{SOA}^{al,G}$ of the SOA needed to provide the gain G. $P_{SOA}^{al,G}$ can be expressed as follows:

$$P_{SOA}^{al,G} = V_b i_b = V_b \left(1 + \frac{lnG}{\Gamma_{SOA} \alpha_{SOA} L_{SOA}} \right) i_t \tag{1}$$

where V_b is the SOA forward bias voltage, i_b is the polarization current, Γ_{SOA} is the confinement factor, α_{SOA} is the material loss, L_{SOA} is the length and i_t is the transparency current given by:

$$i_t = \frac{q w_{SOA} d_{SOA} L_{SOA} N_0}{\tau} \tag{2}$$

where w_{SOA} is the SOA active region effective width, d_{SOA} is the active region depth, $q = 1.6 \times 10^{-9} C$ is the electronic charge, N_0 is the conduction band carrier density required for transparency, τ is the carrier spontaneous decay lifetime.

4.2 Analytical models

The analytical evaluation of the OPS power consumption is carried out as a function of the main switch and traffic parameters (Eramo, 2010; Eramo et al., 2011). We propose two analytical models to evaluate the power consumption of synchronous Optical Packet Switches equipped with Single-Stage and BENES switching fabric in Sections 4.2.1 and 4.2.2 respectively.

4.2.1 Analytical evaluation of the power consumption in SSPN OPS equipped with single-stage fabric switching

In evaluating the various power consumption in the SS-SSPN Optical Packet Switch we notice from Figs 1,6 that at time t:

- there are as many turned on synchronizers in the synchronization stage as the number $N_a(t)$ of packets forwarded;
- there are as many turned on SOAs in 1st stage as the number $N_a(t)$ of packets forwarded;
- the number of turned on SOAs in both 2nd stage and 3rd stage equals the number $N_c(t)$ of converted packets;
- there are as many active turned on SOAs in 4th SSM stage as the number $N_d(t)$ of OFs in which at least one packet is directed;

- all of the r Wavelength Converters are turned on; this assumption is a consequence of the limited speed of each WC that makes no feasible the use of a WC when only a wavelength conversion has to be performed.

According to these remarks we can write the following expression for the average power consumption $P_{av,T}^{SS-SSPN}$ for the SS-SSPN switch:

$$P_{av,T}^{SS-SSPN} = E[N_a]C^{SYN} + E[N_a]C_1^{SOA} + E[N_c](C_3^{SOA} + C_4^{SOA}) + E[N_d]C_2^{SOA} +$$
$$+ rC_{WC} + E[N_{SOA}^{SS-SSPN,off}]C_{off}^{SOA} \qquad (3)$$

wherein:

- C^{SYN} is the power consumption of a turned on synchronizer;
- C_i^{SOA} ($i=1,\ldots,4$) is the power consumption of a turned on SOA in the ith stage ($i=1,\ldots,4$); from Eq. 1 obviously we have $C_i^{SOA} = P_{SOA}^{al,G_i}$ ($i=1,\ldots,4$) where $G_1 = N + r$, $G_2 = NM + r$, $G_3 = NM$ and $G_4 = N$ are the gains needed to overcome the loss for the turned on SOA located in the ith stage ($i=1,\ldots,4$);
- C_{WC} is the power consumption of a Wavelength Converter;
- C_{off}^{SOA} is the power consumption of a turned off SOA; it is equal to $V_b i_{off}$ where i_{off} is the polarization current of an inactive SOA and needed to guarantee a high SOA switching rate (Eramo et al., 2011);
- $E[N_a]$, $E[N_d]$ and $E[N_c]$ are the steady-state average values of the random processes $N_a(t)$, $N_d(t)$ and $N_c(t)$ respectively at an arbitrary epoch; the evaluation of $E[N_a]$, $E[N_d]$ and $E[N_c]$ is carried out in in Appendix-A (Eramo et al., 2008; 2009a;c; 2011);
- $E[N_{SOA}^{SS-SSPN,off}]$ is the number of turned off SOAs; it is given by the total number $N_{SOA}^{SS-SSPN,tot} = N(N+r)M + r + Nr + N$ of SOAs to the total number $N_{SOA}^{SS-SSPN,on} = E[N_a] + 2E[N_c] + E[N_d]$ of turned on SOAs that is:

$$E[N_{SOA}^{SS-SSPN,off}] = N(N+r)M + r + Nr + N - (E[N_a] + 2E[N_c] + E[N_d]) \qquad (4)$$

4.2.2 Analytical evaluation of the power consumption in SSPN OPS equipped with BENES fabric switching

Each 1×2 splitter, 2×2 directional coupler and 2×1 coupler shown in Fig. 10 introduce an attenuation of 2 that is recovered by the SOAs located after each splitter, directional coupler and coupler. If a packet is directly forwarded it goes through the BENES switch once. Conversely if the packet has to be wavelength converted the BENES switch is crossed twice and a wavelength converter is used. In particular notice as a directly forwarded packet needs the use of one 1×2 splitter, one 2×1 coupler, $2log_2 2NM - 2$ directional couplers and $2log_2 2NM$ SOAs each having a gain equal to 2. On the contrary a wavelength converted packet needs the use of two 1×2 splitters, two 2×1 couplers, $4log_2 2NM - 4$ directional couplers and $4log_2 2NM$ SOAs. Let us denote with C_{df}^{SOA} and C_{wc}^{SOA} the sum of the power consumption of the SOAs involved in the switch paths in the case in which a packet is directly forwarded and wavelength converted respectively. We can write the following expression for

the average power consumption $P_{av,T}^{B-SSPN}$ of a SSPN switch equipped with BENES switching fabric:

$$P_{av,T}^{B-SSPN} = E[N_a]C^{SYN} + E[N_a]C_{df}^{SOA} + E[N_c]C_{wc}^{SOA} + rC_{WC} + E[N_{SOA}^{B-SSPN,off}]C_{off}^{SOA} \quad (5)$$

where $E[N_{SOA}^{B-SSPN,off}]$ is the number of turned off SOAs; it is given by the total number $N_{SOA}^{B-SSPN,tot} = 4NMlog_2 2NM$ of SOAs to the total number $N_{SOA}^{B-SSPN,on} = 2(E[N_a] + E[N_c])log_2 2NM$ of turned on SOAs that is:

$$E[N_{SOA}^{B-SSPN,off}] = (4NM - 2(E[N_a] + E[N_c]))log_2 2NM \quad (6)$$

Because the power consumption of turned on SOA in the BENES switching fabric equals $P_{SOA}^{al,2}$, we can simply write the following expression for C_{df}^{SOA} and C_{wc}^{SOA}:

$$C_{df}^{SOA} = 2P_{SOA}^{al,2}log_2 2NM \quad (7)$$

$$C_{wc}^{SOA} = 4P_{SOA}^{al,2}log_2 2NM \quad (8)$$

Finally notice as by inserting Eqs (6)-(8) in Eq. (5) and by using the expressions of $E[N_a]$, $E[N_d]$ and $E[N_d]$ evaluated in Appendix-A (Eramo et al., 2008; 2009a;c; 2011), we can able to calculate the average power consumption $P_{av,T}^{B-SSPN}$ of the synchronous SPN switch equipped with BENES switching fabric.

4.3 Evaluation of power consumption

We compare some Optical Packet Switching architecture by taking into account as reference the average energy consumption per bit $E_{av,T} = \frac{P_{av,T}}{NMB}$ where B denotes the bit rate carried out on each wavelength.

We perform the analysis under the following assumptions:

- the synchronizer described in Fig. 3 is used. Because in each stage and at each time only one of two SOAs is active, assuming a 3 dB attenuation for the couplers and splitters and neglecting the loss occurring in both the OBF and the short FDLs, we have the following expression for the synchronizer's power consumption:

$$P_{SYN} = N_{SYN}P_{SOA}^{al,G} \mid_{G=4} \quad (9)$$

- The SOA's power consumption model illustrated in Section 4.1 is adopted and allowing us, according to Eq. (1), to express the SOA power consumption as a function of the main SOA parameters (V_b, i_b, w_{SOA}, …); A♯2 commercial SOAs Eramo (2010) produced by manufacture A is used to implement the switching fabric. The A♯2 parameter values are reported in Table 1.

- As Wavelength Converter, the Delayed Interference Signal Wavelength Converter (DISC) illustrated in Section 2.2 is used. Its power consumption has been evaluated in (Sakaguchi et al., 2007) when commercial SOA produced by some manufactures are employed. In particular we consider the B♯1 SOA characterized by a Multiple Quantum Well (MQW) type structure and produced by manufacture B. We report in Table 2 the main parameter values for B♯1. The power consumption, measured in (Sakaguchi et al., 2007), is also reported. It equals 187mW when the WC is operating at bit-rate B=40 Gb/s.

Symbol	Explanation	Value
V_b	Forward Bias Voltage	2 V
Γ_{SOA}	Confinement Factor	0.15
α_{SOA}	Material Loss	10^4
L_{SOA}	Length	$700\,\mu m$
w_{SOA}	Active Region Effective Width	$2\,\mu m$
d_{SOA}	Active Region Depth	$0.1\,\mu m$
N_0	Conduction Band Carrier Density	$10^{24}m^{-3}$
τ	Carrier Spontaneous Decay Lifetime	$10^{-9}s$
P_{sat}	Saturation Power	$50\ mW$

Table 1. Main parameter values for the $A\sharp2$ commercial SOAs (Sakaguchi et al., 2007)

	Type	Active region Length (μm)	Active region width (μm)	Active region thickness (μm)	Confinement Factor	Consumed power (mW) (40Gb/s)
B#1	MQW	1100	1,25	0,038	0,2	187

Table 2. Main parameter values for the $B\sharp1$ commercial SOA (Sakaguchi et al., 2007); the power consumption of DISCs realized with $B\sharp1$ SOAs is also reported at bit-rate B=40 Gb/s.

Next, we compare the average energy consumption per bit $E_{av,T}$ of four optical packet switches (OPS) equipped with Single-Stage switching fabric: the Asynchronous Shared-Per-Wavelength (SS-ASPW) and the Asynchronous Shared-Per-Node (SS-ASPN) OPS where the WCs are per wavelength and fully shared respectively, the Synchronous Shared-Per-Wavelength (SS-SSPW) and Synchronous Shared-Per-Node (SS-SSPN) OPSs where the packets are synchronously switched and the WCs are shared per wavelength and per node, respectively. To evaluate power consumption in SS-SSPN OPS, we use the model described in Section 4.2.1. The models described in (Eramo et al., 2009c; Eramo, 2010; Eramo et al., 2011) are used to evaluate the power consumption in SS-ASPN, SS-SSPW and SS-ASPW optical packet switches. Sample switch design is reported in Fig. 11 with target Packet Loss Probability (PLP) smaller than or equal to 10^{-6}. Fig. 11 has been obtained for SS-ASPW, SS-ASPN, SS-SSPN, and SS-SSPW switches by the application of the related models (Eramo et al., 2008; 2009c; Eramo, 2010; Eramo et al., 2011) , for switch size $N = 16$, varying the offered traffic p. The number of wavelengths needed to obtain the asymptotic target PLP value (10^{-6}) is calculated first for each value of the offered load. This number of wavelengths depends on output contention only and therefore is influenced by the choice of operational context (synchronous or asynchronous) and not by the switch architecture. As a consequence, the synchronous solutions require fewer wavelengths to achieve the same PLP target. Then the minimum number of wavelength converters to reach that asymptotic PLP target value (Eramo, 2000) is determined. From Fig. 11 you can notice for a given value of offered traffic, the Shared-Per-Node switch needs fewer WCs than Shared-Per-Wavelength Node. This is obviously due to the full WC sharing strategy adopted in SPN nodes (Eramo et al., 2009b).
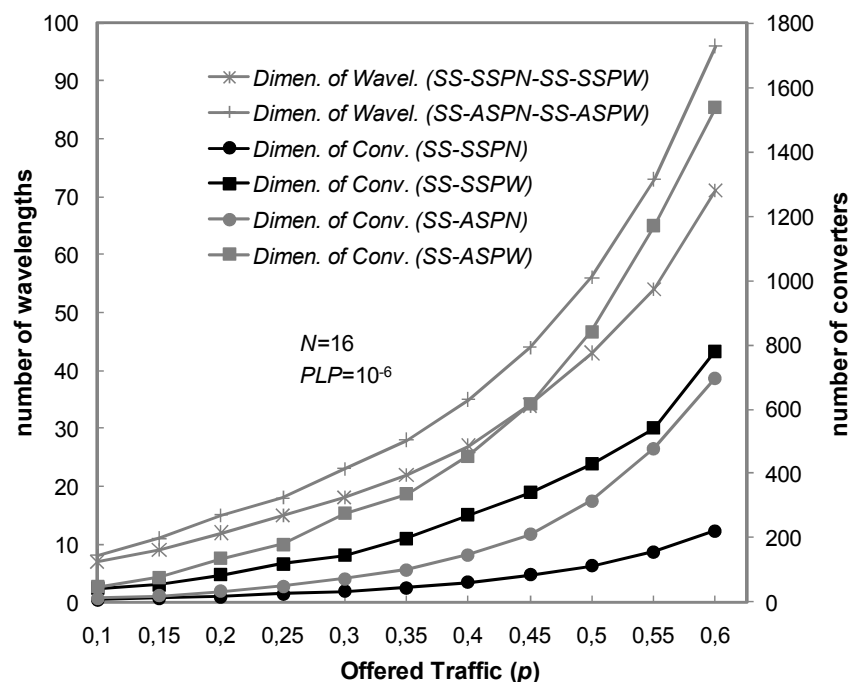
Fig. 11. Dimensioning of wavelengths and WCs in SS-ASPW, SS-ASPN, SS-SSPW and SS-SSPN switches so that the PLP is smaller than or equal to 10^{-6}. The number N of Input/Output Fibers equal 16 and the offered traffic p is varying from 0,1 to 0,6.

In Fig. 12, the average energy consumption per bit $E_{av,T}$ of switch configurations obtained in Fig. 11 as a function of the offered load is presented. Synchronizers with N_{SYN}=4 stages are considered. A bandwidth B=40Gb/s is occupied by each signal. The SS-ASPW architecture presents itself as the most power-efficient solution among all compared solutions as a consequence of the combination of asynchronous operation and wavelength converter sharing solution that allow the use of smaller Space Switching Module in the 1st and 3rd stages that leads to both smaller attenuation and SOA power consumption.

The comparison in power consumption for Synchronous SPN Optical Packet Switches equipped with Single-Stage and BENES switching fabric is reported in Fig. 13 where the average energy consumption per bit $E_{av,T}^{SS-SSPN}$ and $E_{av,T}^{B-SSPN}$ are reported versus the number N of Input/Output Fibers for M=64, N_{SYN}=16 and B=40Gb/s.

The turned off SOAs are polarized with injection current i_{off}=7mA needed to increase the switching rate. In fact the rise-time and the fall-time decrease with increasing injection current because of the strong dependence of the carrier lifetime on the carrier density (Ehrhardt et al., 1993). From Fig. 13 we can notice that for N greater than or equal to 36, $E_{av,T}^{B-SSPN}$ overcomes $E_{av,T}^{SS-SSPN}$ and the BENES switch is more efficient in energy consumption than Single-Stage switch for N increasing. That is a consequence of the linear dependence $O(Nlog_2N)$ of the number of SOA in BENES switch against the quadratic dependence $O(N^2)$ in Single-Stage switch when N increases. This different type of dependence allows a reduction in number of turned off SOAs in BENES switch with respect to the Single-Stage switch. That is confirmed in Fig. 14 where we report the number of turned off SOA versus N in Single-Stage and BENES switches for the same parameters of Fig. 13.
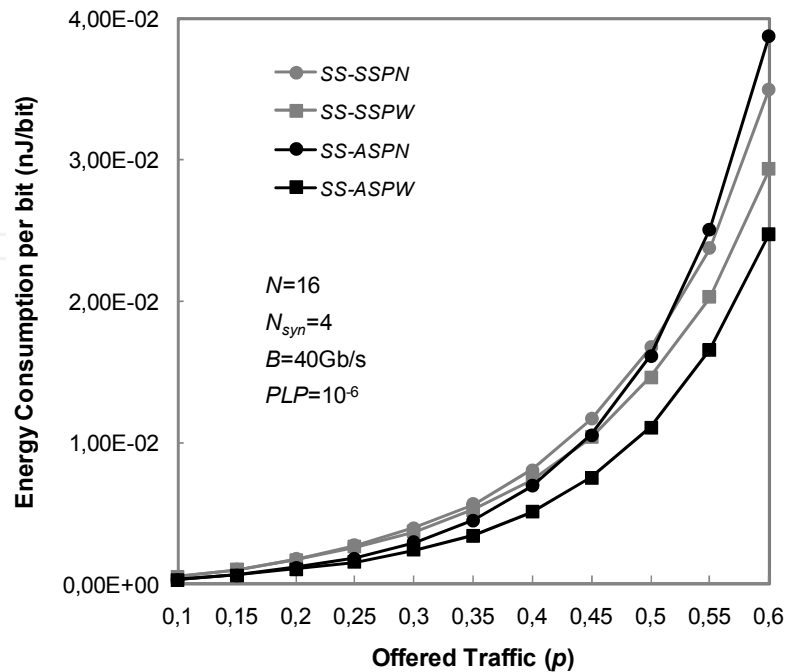
Fig. 12. Average energy consumption per bit in Single Stage(SS) ASPW, ASPN, SSPW and SSPN switches versus the offered traffic for N=16 and N_{SYN}=4. The number M of wavelengths and the number of WCs are dimensioned so that the the PLP is smaller than or equal to 10^{-6}.
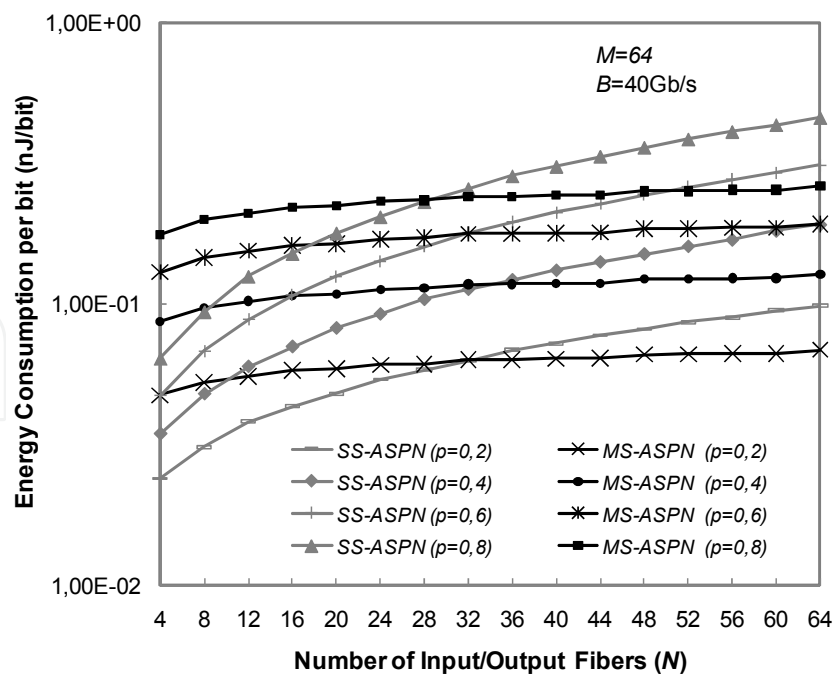

Fig. 13. Comparison of average energy consumption per bit in Single Stage (SS) SSPN and Benes (B) SSPN switches versus the number N of Input/Output Fibers for M=6 and p varying from 0,2 to 0,8. The turned off SOAs are polarized with a current i_{off}=7mA.
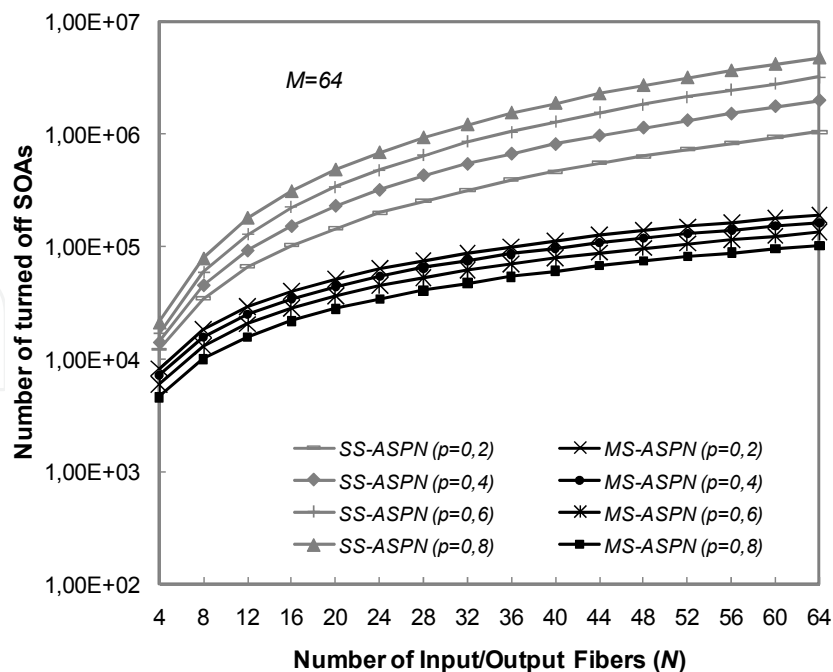
Fig. 14. Number of turned off SOAs in SS-SSPN and B-SSPN switches versus the number N of Input/Output Fibers for M=64. The offered traffic p is varied from 0,2 to 0,8.

5. Conclusions

The chapter discussed issues concerning power consumption of future high-capacity optical packet nodes. When using optical buffers, due to attenuation problems, optical nodes consumes more power than electronic nodes. For this reason we have taken into account bufferless OPS equipped with shared Wavelength Converters to solve output packet contentions. We have proposed some sophisticated analytical models in order to evaluate and compare the power consumption in OPSs equipped with Single-Stage and Multi-Stage switching Fabric. The obtained results show that in the case of OPS equipped with Single-Stage switching fabric, the combination of the asynchronous operation with the wavelength-based system partitioning in Asynchronous Shared-Per-Wavelength OPS leads to significant power saving with respect to the other solutions in the range of interest for switching fabric dimensioning. Finally we have also shown that for larger switches, the BENES switch has an energy consumption lower than the one of an Single-Stage switch if the current injection of the turned off SOAs is considered.

6. Appendix-A: Evaluation of $E[N_a]$, $E[N_d]$ and $E[N_c]$ in switches equipped with single-stage and BENES switching fabric

The evaluation of $E[N_a]$, $E[N_d]$ and $E[N_c]$ in synchronous Optical Packet Switches is carried under the following assumptions:

• packet arrivals on the $N \times M$ input wavelength channels at each time-slot are not dependent on each other;
• packet arrivals occur with probability p on each input wavelength channel;

- the destination of a packet is uniformly distributed over all N OFs, i.e., the probability that an arriving packet is directed to a given OF is equal to $\frac{1}{N}$.

Due to the synchronous operation mode of the SSPN switches, we can evaluate $E[N_a]$, $E[N_d]$ and $E[N_c]$ at a given time-slot.

The average number $E[N_a]$ of forwarded packets can be evaluated by taking into account that the packet loss can be due to either the lack of output wavelength channels or the lack of wavelength converters. We can write:

$$E[N_a] = E[N_o] - E[N_{p,wl}] - E[N_{p,cl}] \tag{10}$$

wherein:

- $E[N_o] = pNM$ is the average number of packets offered to the switch;
- $E[N_{p,wl}]$ is the average number of lost packets due to the lack of output wavelength channels. It is simply given by:

$$E[N_{p,wl}] = N \sum_{j=M+1}^{NM} (j-M) \binom{NM}{j} \left(\frac{p}{N}\right)^j \left(1 - \frac{p}{N}\right)^{NM-j}. \tag{11}$$

- $E[N_{p,cl}]$ is the average number of lost packets due to the lack of WCs. The evaluation of this term has been evaluated in (Eramo et al., 2002; 2009c) by solving an urn problem (Eramo et al., 2002).

The average number $E[N_d]$ of OFs in which at least one packet is directed can be simply expressed as:

$$E[N_d] = N \left(1 - \left(1 - \frac{p}{N}\right)^{NM}\right) \tag{12}$$

Finally the average number $E[N_c]$ of packets forwarded with wavelength conversion can be computed by subtracting the number $E[N_d]$ of packets forwarded without wavelength conversion to the average number $E[N_a]$ of forwarded packets, that is:

$$E[N_c] = E[N_a] - E[N_d] \tag{13}$$

Finally by inserting (10)-(13) in (3) and (5) we are able to evaluate the average energy consumption $E_{av,T}^{SS-SSPN}$ and $E_{av,T}^{B-SSPN}$ of the switches equipped with Single-Stage and BENES switching fabric respectively.

7. Acknowledgment

8. References

Akar, N.; Eramo, V. & Raffaelli, C. (2011). Comparative analysis of power consumption in asynchronous wavelength modular optical switching fabrics. *Optical Switching and Networking*, Vol. 8, No. 3, July 2011, pp. 139-148, ISSN 1573-4277

Aleksic, S (2011). Energy Efficiency of Electronic and Optical Network Elements. *IEEE Journal of Selected Topics in Quantum Electronics*, Vol. 17, No. 2, March/April 2011, pp. 296-308, ISSN 1077-260X

Ben Yoo, S.J. (2011). Energy Efficiency in the Future Internet: The Role of Optical Packet Switching and Optical-Label Switching. *IEEE Journal of Selected Topics in Quantum Electronics*, Vol. 17, No. 2, March/April 2011, pp. 406-418, ISSN 1077-260X

Benes, V.E. (1965). *Mathematical Theory of Connecting Networks*, Academic Publishing, New York.

Chao, H.; Wu, U.; Zhang, Z.; Yang, S.; Wang, L.; Chai, Y.; Fan, J. & Choa, F. (2000). A photonic front-end processor in a WDM ATM multicast switch. *IEEE Journal of Lightwave Technology*, Vol. 8, No. 3, March 2000, pp. 273-285, ISSN 0733-8724

Ehrhardt, A.; Eiselt, M.; Groβkopf, G.; Kuller, L.; Ludwig, W.; Pieper, R.; Schnabel, R. & Weber, H. (1993). Semiconductor Laser Amplifier as Optical Switching Gate. *IEEE Journal of Lightwave Technology*, Vol. 11, No. 8, August 1993, pp. 1287-1295, ISSN 0733-8724

Eramo, V. (2000). Packet Loss in a Bufferless Optical WDM Switch Employing Shared Tunable Wavelength Converters. *IEEE Journal of Lightwave Technology*, Vol. 18, No. 12, December 2000, pp. 1818-1833, ISSN 0733-8724

Eramo, V.; Listanti, M.; Nuzman, C. & Whiting, P. (2002). Optical Switch Dimensioning and the Classical Occupancy Problem. *International Journal Communications Systems*, Vol. 15, No. 2, March/April 2002, pp. 127-141, ISSN 1074-5351

Eramo, V.; Listanti, M.; & Pacifici, P. (2003). A Comparison Study on the Number of Wavelength Converters Needed in Synchronous and Asynchronous All-Optical Switching Architectures. *IEEE Journal of Lightwave Technology*, Vol. 21, No. 2, February 2003, pp. 340-355, ISSN 0733-8724

Eramo, V. (2006). An Analytical Model for TOWC Dimensioning in a Multifiber Optical-Packet Switch. *IEEE Journal of Lightwave Technology*, Vol. 24, No. 12, December 2006, pp. 4799-4810, ISSN 0733-8724

Eramo, V.; Germoni, A.; Savi, M. & Raffaelli, C. (2008). Multifiber Shared-Per-Wavelength All-Optical Switching: Architectures, Control, and Performance. *IEEE Journal of Lightwave Technology*, Vol. 26, No. 5, March 2008, pp. 537-551, ISSN 0733-8724

Eramo, V.; Germoni, A.; Savi, M. & Raffaelli, C. (2009). Packet loss analysis of shared-per-wavelength multi-fiber all-optical switch with parallel scheduling. *Computer Networks*, Vol. 53, No. 2, February 2009, pp. 202-216, ISSN 1389-1286

Eramo, V.; Germoni, A.; Cianfrani, A.; Savi, M. & Raffaelli, C. (2009). Loss Analysis of Multiple Service Classes in Shared-per-Wavelength Optical Packet Switches. *IEEE/OSA Journal of Optical Communications and Networking*, Vol. 1, No. 2, July 2009, pp. A69-A80, ISSN 1943-0620

Eramo V. & Listanti M. (2009). Power Consumption in Bufferless Optical Packet Switches in SOA Technology. *IEEE/OSA Journal of Optical Communications and Networking*, Vol. 1, No. 3, August 2009, pp. B15-B29, ISSN 1943-0620

Eramo V. (2010). Comparison in Power Consumption of Synchronous and Asynchronous Optical Packet Switches. *IEEE Journal of Lightwave Technology*, Vol. 28, No. 5, March 2010, pp. 847-857, ISSN 0733-8724

Eramo, V.; Germoni, A.; Cianfrani, A.; Listanti, M. & Raffaelli, C. (2011). Evaluation of Power Consumption in Low Spatial Complexity Optical Switching Fabrics. *IEEE Journal of Selected Topics in Quantum Electronics*, Vol. 17, No. 2, March/April 2011, pp. 396-405, ISSN 1077-260X

Hinton, K.; Rakutti, G.; Farrel, P.; & Tucker, R.S. (2008). Switching Energy and Device Size Limits on Digital Photonic Signal Processing Technologies. *IEEE Journal of Selected Topics in Quantum Electronics*, Vol. 14, No. 3, May/June 2008, pp. 938-945, ISSN 1077-260X

Kalman, R.F.; Kazovsky, L.G. & Goodman J.W. (1992). Space Division Switches Based on Semiconductor Optical Amplifiers. *IEEE Photonic Technology Letters*, Vol. 4, No. 9, September 1992, pp. 1048-1051, ISSN 1045-1135

Mack, J.P.; Poulsen, H.N. & Blumenthal D.J. (2008). Variable Length Optical Packet Synchronizer. *IEEE Photonic Technology Letters*, Vol. 20, No. 14, July 2008, pp. 1252-1254, ISSN 1045-1135

Okada, A.; Sakamoto, T.; Sakai, Y.; Noguchi, K. & Matsuoka M. (2001). All-optical packet routing by an out-of-band optical label and wavelength conversion in a full-mesh network based on a cyclic-frequency AWG, *Proceedings of OFC 2001*, pp. ThG5, S. Diego (CA), March 2001

Sabella, R.; Listanti, M. & Eramo V. (2000). Architectural and technological issues for future optical Internet networks. *IEEE Communications Magazine*, Vol. 38, No. 9, September 2000, pp. 82-92, ISSN 0163-6804

Sakaguchi, J.; Salleras, F.; Nishimura K. & Ueno Y. (2007). Frequency-dependent Electric dc Power Consumption Model Including Quantum-Conversion Efficiencies in Ultrafast All-Optical Semiconductor Gates around 160 Gb/s. *Optics Express*, Vol. 15, No. 10, October 2007, pp. 14887-14900, ISSN 1094-4087

Sakamoto, T.; Okada, A.; Hirayama M.; Sakai Y.; Morikawi O.; Ogawa I.; Sato R.; Noguchi K. & Matsuoka M. (2002). Optical Packet Synchronizer using Wavelength and Space Switching. *IEEE Photonic Technology Letters*, Vol. 14, No. 9, June 2002, pp. 1360-1362, ISSN 1045-1135

Tucker, R.S. (2011). Green Optical Communications-Part II: Energy Limitations in Networks. *IEEE Journal of Selected Topics in Quantum Electronics*, Vol. 17, No. 2, March/April 2011, pp. 261-274, ISSN 1077-260X

Zucchelli, L.; Bella, D.; Fornuto, G.; Gambini, P.; Re, D.; Delorme, F.; Kraehenbuehl R. & Melchior, H. (1998). An experimental optical packet synchronizer with 100 ns range and 200 ps resolution, *Proceedings of ECOC 1998*, pp. 587-588, Madrid (Spain), September 1998
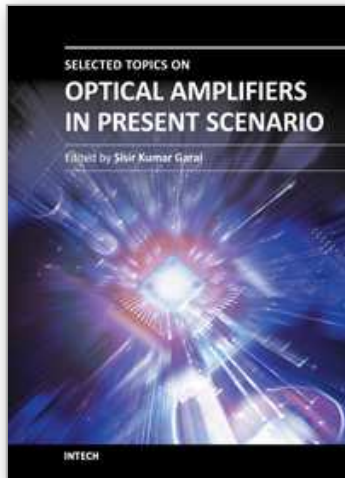
Selected Topics on Optical Amplifiers in Present Scenario

Edited by Dr. Sisir Garai

With the explosion of information traffic, the role of optics becomes very significant to fulfill the demand of super fast computing and data processing and the role of optical amplifier is indispensable in optical communication field. This book covers different advance functionalities of optical amplifiers and their emerging applications such as the role of SOA in the next generation of optical access network, high speed switches, frequency encoded all-optical logic processors, optical packet switching architectures, microwave photonic system, etc. Technology of improving the gain and noise figure of EDFA and, the study of the variation of material gain of QD structure are also included. All the selected topics are very interesting, well organized and hope it will be of great value to the postgraduate students, academics and anyone seeking to understand the trends of optical amplifiers in present scenario.

How to reference

In order to correctly reference this scholarly work, feel free to copy and paste the following:

V. Eramo, E. Miucci, A. Cianfrani, A.Germoni and M. Listanti (2012). SOA-Based Optical Packet Switching Architectures, Selected Topics on Optical Amplifiers in Present Scenario, Dr. Sisir Garai (Ed.), ISBN: 978-953-51-0391-2, InTech, Available from: http://www.intechopen.com/books/selected-topics-on-optical-amplifiers-in-present-scenario/soa-based-optical-packet-switching-architectures

INTECH
open science | open minds